

A Study of Neutral V Particles*

W. B. FRETTER, M. M. MAY, AND M. P. NAKADA

Department of Physics, University of California, Berkeley, California

(Received September 15, 1952)

The V particles produced in penetrating showers have been studied in a cloud chamber containing lead plates. The results can be interpreted in terms of two types of neutral unstable particles, $V_1^0 \rightarrow p + \pi$ and $V_2^0 \rightarrow \pi + \pi$, although other possibilities are not excluded by our data. Analysis of the dynamics of three-particle decay indicates that such a process must still be considered as possible. The lifetimes of the particles have been calculated, taking into account the bias introduced by the finite size of the cloud chamber. If we use average values for the masses of the unstable particles, the lifetime for the V_1^0 is $(10 \pm 7) \times 10^{-10}$ sec and for the V_2^0 is $(4 \pm 3) \times 10^{-10}$ sec.

INTRODUCTION AND APPARATUS

THE unstable particles produced in penetrating showers, first discovered by Rochester and Butler in 1947,¹ have now been observed in several laboratories.²⁻⁶ A large cloud chamber formerly used for studies of penetrating showers⁷ was arranged for detection of these unstable neutral particles, called V^0 particles, and has been operated at Berkeley since February, 1950 and at Lake Sabrina, California (9000 feet elevation) during the summer of 1951. We are reporting on about 75 V^0 particles that have been observed to date in this cloud chamber, which has no magnetic field but contains lead plates.

Although the arrangement of the lead plates was changed from time to time, many of the pictures were taken with seven $\frac{1}{2}$ -inch lead plates in the chamber. The plates were spaced about 2 inches apart to allow room for observation of the decaying particles. The arrangement of apparatus is shown in Fig. 1. The chamber was expanded when one and only one of the counters above the chamber triggered in coincidence with both the counters below the chamber. During most of the time there was only a thin roof above the apparatus and nearly all the V^0 particles were created in the material in the chamber. At sea level the counting rate is 2 per hour, with about 2 or 3 penetrating showers per day. The anticoincidence arrangement of the upper counters eliminated many low energy showers which otherwise would have counted in the rather loose selection of events. It seems important not to require very high energy penetrating showers, since the tracks of V^0 particles often may be lost in the large electronic cascades usually accompanying such events.

Stereoscopic pictures were taken with a double lens camera 220 cm in front of the cloud chamber. The lenses were 11.5 cm apart and set at angles of 3° to converge

on the chamber. The pictures were searched for unstable particles in a stereoscopic viewer, and if one was found, measurements on it were made in a reprojection apparatus made especially for the purpose. Examples of V^0 particles photographed with our apparatus have been published.⁸

MEASUREMENTS

The reprojector was designed to give a three-dimensional reproduction of events as they actually took place in the cloud chamber. The same camera that took the pictures was used as a projector, and the film was placed in the same orientation that it had when the pictures were taken. A ground glass plate 60 cm in diameter was used for a screen. A glass plate similar to the front glass of the cloud chamber was mounted in front of the screen to compensate for distortions introduced by photographing through the front plate of the cloud chamber. The screen could be moved toward or away from the camera. It was mounted on swivels so that it could be moved to any possible plane with the center of the screen remaining fixed as the screen was tilted. Because the center of the screen was the fixed reference point in reprojection, the camera mounting was made so that the camera could be moved vertically and horizontally. This allowed the operator to bring any image point within the cloud chamber to focus at the center of the screen.

In reprojecting pictures the following procedure was used. The screen was brought to a position corresponding to the front of the plates of the cloud chamber, and the film was adjusted until the two images of the plates coincided on the screen. The penetrating shower was located and the center of the shower was brought to focus at the center of the screen. This involved motion of the camera vertically and horizontally, motion of the screen toward and away from the camera, and the superposition of the images of penetrating particle tracks which emerged from the penetrating shower center. The latter operation required the tilting of the plane of the screen. With the center of the shower at the

* Assisted by the joint program of the ONR and AEC.

¹ G. D. Rochester and C. C. Butler, *Nature* **160**, 855 (1947).

² Armenteros, Barker, Butler, and Cachon, *Phil. Mag.* **62**, 1113 (1951).

³ Seriff, Leighton, Hsiao, Cowan, and Anderson, *Phys. Rev.* **78**, 290 (1950).

⁴ Thompson, Cohn, and Flum, *Phys. Rev.* **83**, 175 (1951).

⁵ H. S. Bridge and M. Annis, *Phys. Rev.* **82**, 445 (1951).

⁶ W. B. Fretter, *Phys. Rev.* **83**, 1053 (1951).

⁷ W. B. Fretter, *Phys. Rev.* **76**, 511 (1949).

⁸ C. C. Butler, "Unstable Heavy Cosmic Ray Mesons," in J. G. Wilson, *Progress in Cosmic Ray Physics* (North-Holland Publishing Company, Amsterdam, 1952).

center of the screen, an attempt was next made to orient the plane of the screen to see if it could be made to coincide with the plane of the V^0 particle. Sometimes the plane of the V^0 particle did not include the penetrating shower center. In such noncoplanar cases, no angle measurements could be made. When the plane of the V^0 particle contained the center of the penetrating shower, angle measurements were made as follows.

A line through the penetrating shower origin and the apex of the V^0 particle was used as reference, and the angles that the decay products made with this line were measured. The distance between the origin of the penetrating shower and the apex of the V^0 particle was measured, and the maximum available distance in the cloud chamber for the detection of each V^0 particle was measured along the same reference line. The position of the event within the chamber was noted. The angle between the initiator of the penetrating shower and the reference line was measured. The angle between the plane containing the V^0 and the plane containing the reference line and the initiating particle was estimated. Figure 2 shows the most important quantities measured.

The ionization of the tracks was estimated by making comparisons with minimum ionizing particle tracks. Scattering of tracks in the plates of the chamber was also measured. Ionization and scattering were also

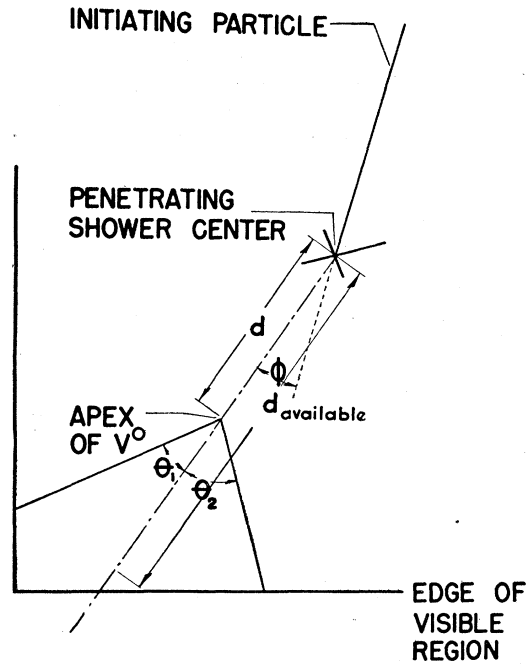


FIG. 2. Sketch showing some of the quantities measured in a picture of a V^0 particle.

observed with the viewer and from positive enlarged photographs.

Repeated measurements of the depth position of a penetrating shower center fell within a range of 0.4 cm. Horizontal and vertical positions of the penetrating shower center could usually be located to ± 0.1 and ± 0.2 cm, respectively, depending on the number and geometry of unscattered penetrating particles in the penetrating shower. The accuracy of measurements on particles depended on the orientation of the event, the distance from and orientation with respect to the penetrating shower center, and the lengths of unscattered track available for measurement. Measurements on how closely the plane of the V^0 event contained the penetrating shower center were made as follows. The penetrating shower center was moved to different off-coincidence positions, and the plane of the screen was reoriented to see if the V^0 images could be made to coincide. Then, with the origin of the penetrating shower in coincidence, different screen orientations were tried to determine when the V^0 event went out of coincidence. With certain events 2° shifts in the plane would result in noncoincidence. Most events were such that 5° shifts in planes would result in noncoincidence.

IDENTIFICATION OF V PARTICLES

Although it seems well established now that most V events are caused by unstable heavy particles, we have made a statistical study of V^0 events that occurred in the gas and in the lead plates of the cloud chamber in a series of 16,570 pictures taken when the chamber contained seven $\frac{1}{2}$ -inch lead plates. A total of 855 pene-

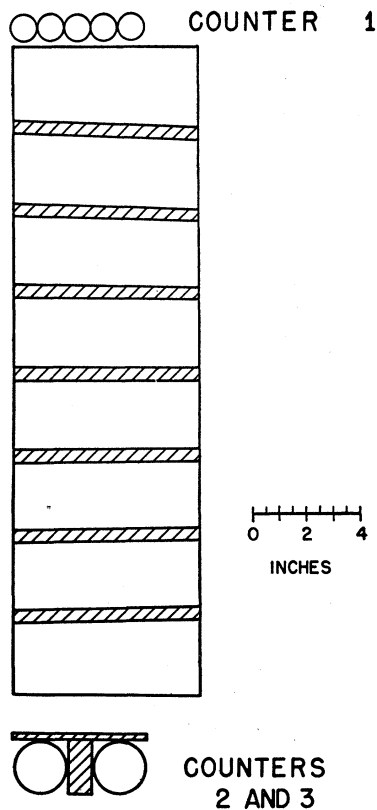


FIG. 1. Schematic diagram of the cloud chamber and counter arrangement.

trating showers occurred in this series, two of which originated in the gas. The number expected to originate in the gas, assuming geometric cross sections, was 1.8.

The V^0 events observed in the gas fell into two sharply distinguished categories. Thirty-eight events were seen in which at least one of the tracks was at four times minimum ionization or less. No track from events in this category terminated in the gas of the chamber. Four events were seen in which both tracks were at least ten times minimum ionization. All but one track from events in this category terminated in the gas.

There was one neutral produced 5-prong star in the gas. There were two stars produced by charged particles in the gas, one with two prongs and one with five prongs, and there was one ten-prong star in which the producer could not be identified.

A total of 26 nonelectronic V^0 events were observed in the lead, and 14 Y events, i.e., a charged particle entering the plate and two nonelectronic charged particles leaving the plate. A very large number of electronic V events and Y events were, of course, observed coming from the lead. Events were called nonelectronic only if the particles penetrated further lead plates without multiplication.

Events whose cross sections are proportional to the geometrical cross section should occur about 500 times more frequently in the lead than in the argon gas. Thus, one would expect $26/500=0.05$ V^0 events and $14/500=0.03$ Y events of this kind in the gas. It is probable, however, that the four very low energy V events are actually neutron stars. No comparison with similar events in the lead can be made in this case, since the particles would not have emerged from the lead plates. It seems clear, however, that the 38 V^0 events of higher energy must originate in decay rather than collision processes. Some of the V events occurring in the lead must also be true V^0 particles, but these have not been included in the analysis.

TABLE I. Statistics of V^0 particle penetrating showers.

	V^0 producing showers	Per-cent	All showers	Per-cent
Charged primary	35	55	620	72
Neutral primary	3	5	46	5
Unknown primary	25	40	192	23
Multiplicities of penetrating particles	4.9 ± 1.2		4.4 ± 1.0	
Large showers	16%		14%	
Showers with only one penetrating particle	14%		5%	
Number of penetrating particles per V^0			80 ± 24	
Number of penetrating showers per V^0			18 ± 3	
Number of V^0 's per calendar month				
Lake Sabrina			16	
Berkeley			2	
Penetrating particles per penetrating shower				
Lake Sabrina			4.4 ± 1.0	
Berkeley			4.3 ± 1.0	

COPLANARITY

It was possible to determine the coplanarity of 63 V^0 particles observed during the course of the experiment. Of these, 43 were coplanar as determined from the reprojector, 13 looked coplanar in the stereoscopic viewer (for various reasons they could not be reprojected) and 7 events were noncoplanar. Only those events were used where the penetrating shower origin was obvious.

If one assumes that all events are due to two-particle decay but that scattering might have taken place before decay to produce the noncoplanar events, a scattering mean free path can be estimated. The total amount of lead traversed by all V^0 's is 1416 g/cm^2 of lead. If the coplanar events did not scatter and the noncoplanar events experienced single scattering only, a scattering mean free path of $200 \pm 90 \text{ g/cm}^2$ of lead is calculated. In estimating the amount of lead traversed by noncoplanar V^0 's, a most likely path with scattering in lead was assumed. Estimated angles of scatter were 10, 20, 30, 45, 70, 90, and 90 degrees.

Various three-particle decay schemes have been suggested.⁹ These would require the decay into two oppositely charged particles and a neutral particle. The most easily identifiable neutral particle is the neutral meson. Its rapid decay into photons of high energy would result in the development of electron showers in the lead plates of the cloud chamber. No showers that might have been the result of the neutral meson were seen, although the usual electronic component in penetrating showers often made the observation uncertain.

From observations of scattering in the lead plates, ionization, and range, it is sometimes possible to make tentative identification of the decay products.¹⁰ As is generally the case in such identification, errors in ionization estimates and poor statistics on scattering measurements combine to make the estimate of mass in an individual case quite uncertain. However, it is usually possible to distinguish a proton from a meson when they are above minimum ionization. In three pictures both tracks could be identified by the above procedures. These were all proton+meson decay events. In other pictures, only one of the particles could be identified: 4 were protons and 7 were mesons.

The penetrating showers in which V^0 's were produced were examined and compared with all penetrating showers detected with the present apparatus to see if any trends could be noticed. The results are given in Table I.

Large showers have been arbitrarily defined as having 8 or more penetrating particles. The corresponding entries mean that, for example, 16 percent of the V^0 producing showers were large showers. Detection efficiency has been ignored, but it is obviously easier to see

⁹ Leighton, Wanlass, and Alford, Phys. Rev. **83**, 843 (1951).

¹⁰ W. M. Powell, Phys. Rev. **69**, 385 (1946).

V particles in small showers than in complicated large showers.

There seem to be no definite trends. Neutral as well as charged primaries produce events that yield V^0 's. Both large and small showers give rise to V^0 's. In two nuclear interactions that gave rise to V^0 's, no penetrating particles were produced directly. In two other pictures, V^0 's were accompanied by one other penetrating track. Nothing else of the same age as the V^0 track appeared in the chamber.

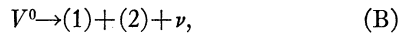
THE DYNAMICS OF DECAY

Before we proceed to an analysis of the data obtained, we will discuss briefly the dynamics of two-particle and three-particle decay in terms of our measurable quantities, which are somewhat different than those measured when the cloud chamber is in a magnetic field. The nature of the unstable neutral particle and the characteristics of the decay products are still not known exactly, and various possibilities must be considered.

The simplest types of decay schemes that may be assumed are the following:



where (1) and (2) are charged particles of opposite signs and of mesonic mass or heavier; and



where ν is a neutrino, so chosen because the near coplanarity of the V^0 with its decay products would seem to rule out the emission of a heavier neutral particle, and the emission of a γ -ray is rendered unlikely by the lack of such observed secondary interactions as would normally accompany it. Of course, there may well be several different V^0 's and several competing modes of decay. As a matter of fact, it is necessary to make an assumption of this kind to interpret existing data.

A. Two-Particle Decay

The dynamics of the two-particle decay process (A) are very simple and have already been discussed extensively in print.^{3,8} The three particles involved must lie in a plane for momentum to be conserved, and, in the rest system of the V^0 , the angle ϕ^* which the (equal and opposite) momenta of particles (1) and (2) make with the direction of the V^0 must be sinusoidally distributed:

$$F(\phi^*)d\phi^* = \sin\phi^*d\phi^*.$$

For completeness, and in order to fix the nomenclature, we list the conservation equations (the velocity of light $c=1$ throughout this paper). m and p refer to the mass and momentum of the V^0 .

(1) In the center-of-mass system of the V^0 :

$$p_1^* = p_2^* = p^*; \quad m = (m_1^2 + p^{*2})^{\frac{1}{2}} + (m_2^2 + p^{*2})^{\frac{1}{2}}.$$

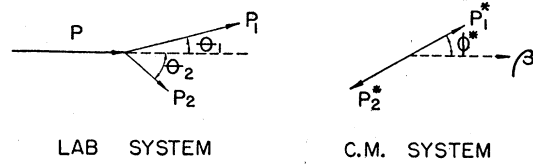


FIG. 3. Momentum vectors in two-particle decay.

(2) In the laboratory system:

$$p = p_1 \cos\theta_1 + p_2 \cos\theta_2; \quad p_1 \sin\theta_1 = p_2 \sin\theta_2;$$

$$(m^2 + p^2)^{\frac{1}{2}} = (m_1^2 + p_1^2)^{\frac{1}{2}} + (m_2^2 + p_2^2)^{\frac{1}{2}}.$$

See Fig. 3. Once values for the masses are chosen, there are only two independent variables, which may be taken to be p_1 , p_2 , or θ_1 , θ_2 or ϕ^* , γ , where $\gamma = (1 - \beta^2)^{-\frac{1}{2}}$, $\beta =$ velocity of the V^0 . The relativistic transformation equations for the angles are

$$\cot\theta_1 = \gamma \left(\cot\phi^* + \frac{\beta}{\beta_1^*} \csc\phi^* \right);$$

$$\cot\theta_2 = \gamma \left(-\cot\phi^* + \frac{\beta}{\beta_2^*} \csc\phi^* \right).$$

These equations underlie much of the development which is to follow (they are valid, of course, no matter what the decay scheme). They can also give some insight into the behavior of θ_1 and θ_2 , which are important quantities for our analysis.

It is also seen that, if $\beta > \beta_1^*$, then θ_1 is acute for all values of ϕ^* , its maximum value being

$$\cot\theta_1 = (\gamma\beta/\beta_1^*)(1 - \beta_1^{*2}/\beta^2)^{\frac{1}{2}},$$

which is near the most probable value for $\beta \gg \beta_1^*$. Similar considerations apply to β_2^* and θ_2 . The total opening angle θ is also restricted in range for certain β 's, and curves exhibiting its variation with ϕ^* are given by Butler.⁸

In order to discuss what use may be made of those results, the experimental apparatus must be considered. The apparatus now in use in various laboratories differs as follows: (1) a magnetic field may or may not be present; (2) the initial event giving rise to the V^0 can or cannot be located. If a magnetic field is present, (Leighton *et al.*;⁹ Manchester group²), independent estimates of m_1 and m_2 can be made, using track ionizations. Those estimates are usually compatible with the identification of (1) and (2) with known particles (protons and π -mesons), within the error inherent in the ionization measurements. One can then obtain the mass of the V^0 in terms of p_1 , p_2 , and θ .² If the initial event can be located, the two-particle decay assumption may be tested directly by checking the coplanarity of the V^0 with the center of the initial event, as well as the transverse momentum balance.

Granting that the observations are found to be at least partially fitted by one or more two-particle decay

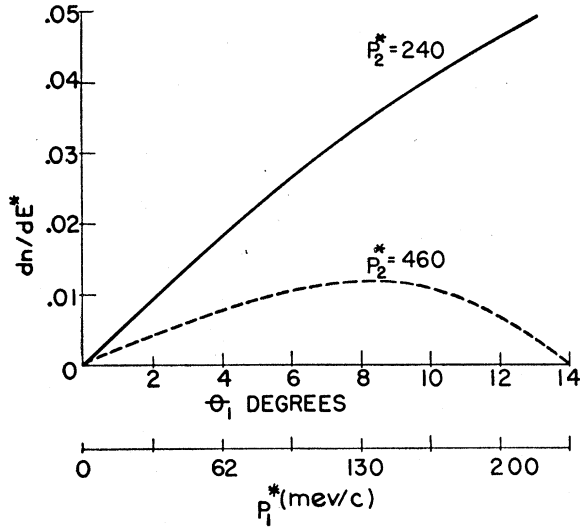


FIG. 4. Distribution functions for the momentum of the proton in three-particle decay.

schemes, the distribution in ϕ^* may be obtained and compared with the theoretical sinusoidal distribution. If the initial event is not located (θ_1, θ_2 not known), one may use

$$\sin\phi^* = p_1 p_2 \sin\theta / p p^*.$$

If there is no magnetic field, but the initial event can be located, the only measurable quantities of the ones which occur in the conservation equations are θ_1 and θ_2 . One must therefore assume, *a priori*, one or more reasonable decay processes. The number of such processes is restricted by the coplanarity property and by the characteristics of the decay tracks (penetration, ionization, etc.). If one makes the simplest plausible assumption of a V^0 decaying into two known charged particles only, the V^0 mass becomes the only adjustable parameter, and one has two criteria with which to make the adjustment: the distribution in ϕ^* and the observed ionizations of the decay tracks. In terms of θ_1 and θ_2 , these quantities are given by¹¹

$$\cos^2\phi^* = \frac{1 + \delta^2 + 1/\sigma^2 - [(1 + \delta^2 + 1/\sigma^2)^2 - 4\delta^2]^{\frac{1}{2}}}{2},$$

where

$$\delta = \frac{1/\beta_2^* - K/\beta_1^*}{1 + K}, \quad K = \frac{\tan\theta_1}{\tan\theta_2}, \quad \sigma = \frac{\cot\theta_1 + \cot\theta_2}{1/\beta_1^* + 1/\beta_2^*},$$

and the sign of $\cos\phi^*$ is the same as the sign of δ ;

$$\beta_1 = \frac{\sin\phi^*/\sin\theta_1}{[m_1^2/p^{*2} + \sin^2\phi^*/\sin^2\theta_1]^{\frac{1}{2}}} \quad (\text{similarly for } \beta_2).$$

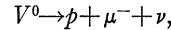
β_1^* , β_2^* and p^* are, of course, functions of m , m_1 , m_2 only.

¹¹ M. M. May, Ph.D. thesis, University of California, 1952 (unpublished).

In addition, the decay tracks may undergo ionization changes, scattering, and other significant interactions. In particular, a track may stop within a known thickness of lead, thus allowing an upper limit to be set on p_1 or p_2 as the case may be. The other momentum is then obtained from transverse momentum conservation, and an upper limit for m , the V^0 mass, can be calculated by the formula given above. If the track penetrates one or more plates before stopping (but suffers no nuclear interactions), both an upper and a lower limit for m may be found.

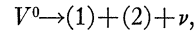
B. Three-Particle Decay

One is led to the assumption of three-particle decay for the V^0 mainly by the impossibility of explaining the experimental data by means of a single two-particle decay process, since the energy available in the center-of-mass system of the V^0 does not have a unique value. As an alternative to postulating the existence of two types of V^0 's, with what turns out to be similar lifetimes and frequency of production but different masses, decay products, and possibly different spins, the hypothesis of a single V^0 with a single three-particle decay has been advanced.¹² The third particle is taken to be a neutrino. The particular decay scheme,



may be thought attractive in the light of the fact that a lifetime of 10^{-10} second yields very closely the coupling constant for Fermi interactions,⁶ and this scheme has been used as a numerical example in what follows. Replacing the μ^- means by a π^- makes very little difference quantitatively.

We consider first the general process



(1) and (2) being massive particles. Obviously, it is impossible to draw exact conclusions as to angular and momentum spectra without a detailed interaction theory. Still, one may expect to observe any sharply varying functional dependences of the phase space factor in the transition rate formula on observable quantities:

$$\frac{dn}{dE} = \frac{2}{\pi\hbar^3} \frac{p_1^2 dp_1 p_2^2 dp_2}{dE} d\Omega_1 d\Omega_2.$$

We proceed to look for such variations. We shall work first in the center-of-mass system of the V^0 , where we note that (a) there are two independent variables relevant to the decay process, as the momentum triangle can be specified by three variables and the energy equation makes one of them a function of the other two; we choose for these variables p_1^* and p_2^* , the momenta of (1) and (2) in the center-of-mass system; (b) in the

¹² K. A. Brueckner and R. W. Thompson, Phys. Rev. 87, 390 (1952). T. D. Lee, private communications.

elements of solid angle $d\Omega_1 d\Omega_2$, there is only one angle which affects physically significant quantities in the center-of-mass system; the others specify the position of the momentum triangle in space; we choose for that angle θ^* , the angle between p_1^* and p_2^* , and lump the others into the symbol $d\Omega'$, so that $d\Omega_1 d\Omega_2 = \sin\theta^* d\theta^* d\Omega'$.

The conservation equations for energy and momentum yield

$$\cos\theta^* = [(E^* - E_1^* - E_2^*)^2 - p_1^{*2} - p_2^{*2}] / 2p_1^* p_2^*,$$

where

$$E_1^* = (m_1^2 + p_1^{*2})^{1/2}; \quad E_2^* = (m_2^2 + p_2^{*2})^{1/2}.$$

E^* , the total energy available, $=m$, the V^0 mass. Then

$$d(\cos\theta^*)/dE^* = (E^* - E_1^* - E_2^*)/p_1^* p_2^*,$$

and

$$\frac{dn}{dE^*} = \frac{2}{\pi\hbar^3} p_1^* p_2^* (E^* - E_1^* - E_2^*) dp_1^* dp_2^* d\Omega'.$$

As a function of p_1^* , this expression vanishes at $p_1^* = 0$ and at $E_1^* = E^* - E_2^*$. The latter limit corresponds to the largest value which p_1^* can take on for any p_2^* . However, p_2^* is an independent variable, and, for a given p_2^* , p_1^* can only range from 0 to

$$[(E^* + p_2^* - E_2^*)^2 - m_1^2] / 2(E^* + p_2^* - E_2^*).$$

Thus, if we plot a set of curves of dn/dE^* vs p_1^* , each curve corresponding to one value of p_2^* , dn/dE^* is seen not to vanish when p_1^* reaches its upper limit as determined by the conservation equations, except on the curve defined by

$$p_2^* = \left[\frac{(m^2 - m_1^2 - m_2^2)^2 - 4m_1^2 m_2^2}{4m^2} \right]^{1/2}.$$

For that case, in the upper limit $p_1^* = p_2^*$, no neutrino is emitted, and the momenta of both (1) and (2) reach their largest possible values. Such a curve is plotted in Fig. 4 (dotted line) for a plausible set of values of m , m_1 , m_2 . A curve corresponding to a lower, and more probable value of parameter p_2^* is also shown (full line). For that case, we see that not only does dn/dE^* not vanish when p_1^* reaches its upper limit, but the upper limit is reached before dn/dE^* passes through its maximum, a maximum which occurs when p_1^* satisfies

$$E_1^* + p_1^{*2}/E_1^* = E^* - E_2^*.$$

We proceed to use these results to obtain a distribution in θ_1 , the angle which the proton in the laboratory system makes with the V^0 (see Fig. 5). For not too slow V^0 's, this angle is expected to be small, because p_1^* , p_2^* , and p_v^* will tend to be approximately equal (on the basis of phase space considerations only), making the velocity of the proton in the center-of-mass system, β_1^* , small, and its (vector) velocity in the laboratory system, β_1 , not very different from the velocity of the

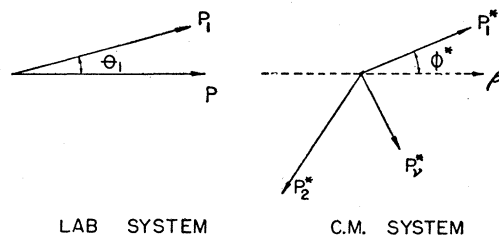


FIG. 5. Momentum vectors in three-particle decay.

V^0 , β . The Lorentz transformation on angles gives

$$\tan\theta_1 = \frac{p_1^* \sin\phi^*}{\gamma(p_1^* \cos\phi^* + \beta E_1^*)} = \frac{\sin\phi^*}{\gamma(\cos\phi^* + \beta/\beta_1^*)},$$

where the nomenclature is taken over unchanged from the discussion of two-particle decay (see Fig. 3). We note again that $\tan\theta_1$ increases monotonically with β_1^* , but, as a function of ϕ^* , reaches a maximum at $\cos\phi^* = -\beta_1^*/\beta$. Since, as we have seen, β_1^* possesses an upper limit corresponding to $E_1^* = E^* - E_2^*$ and depending only on the values of the masses, there exists a similar upper limit to $\tan\theta_1$. Choosing $m = 2400$ electron masses (on the high side of the plausible range), $m_1 = 1836$ and $m_2 = 210$ gives

$$\tan\theta_1 \leq \frac{0.25}{\gamma\beta} \frac{1}{(1 - (0.25/\beta)^2)^{1/2}}.$$

At this point, we introduce a nonrelativistic approximation for p_1^* and E_1^* , since all evidence points to a disintegration energy small (10–20 percent) compared with the proton mass. In order to obtain the distribution function in terms of θ_1 and ϕ^* , it must be noted that five independent variables are needed to specify the momenta and the angles between them in the laboratory system. Those variables may be taken to be p_1^* , p_2^* (or alternately θ_1 , p_2^*), β , ϕ^* , and ψ , where ψ is the angle between the plane containing p_1^* , p_2^* , and p_v^* and the plane containing p_1^* and β . The symbol $d\Omega'$ which occurs in the expression for dn/dE^* can be written out explicitly:

$$d\Omega' = 2\pi \sin\phi^* d\phi^* d\psi,$$

where the 2π comes from integration over an angle expressing rotation of the entire figure about the direction of the V^0 as an axis. We then have

$$\begin{aligned} \frac{dn}{dE^*} &= \frac{4}{\hbar^3} \gamma^2 \beta^2 m_1^2 p_2^* \frac{\tan\theta_1 \sec^2\theta_1 \sin^2\phi^*}{(\sin\phi^* - \gamma \tan\theta_1 \cos\phi^*)^3} \\ &\times \left[E^* - E_2^* - m_1 - \frac{1}{2}m_1 \left(\frac{\gamma\beta \tan\theta_1}{\sin\phi^* - \gamma \tan\theta_1 \cos\phi^*} \right)^2 \right] \\ &\times d\theta_1 d\phi^* dp_2 d\psi. \end{aligned}$$

The corresponding relativistic expression has been calculated.¹¹ A representative plot may perhaps be ob-

TABLE II. Observed and calculated data for 34 coplanar measurable V^0 decays.

$p+\pi$ $m=2210$	No.	θ_1	θ_2	$I_1 \text{ obs}/$ I_{min}	$I_2 \text{ obs}/$ I_{min}	Identi- fication (1) (2)	d cm	d_a cm	ϕ	ϕ^*	$I_1 \text{ calc}/$ I_{min}	$I_2 \text{ calc}/$ I_{min}	γ	$t \times 10^{10}$	$t_a \times 10^{10}$
	38,789	9	27	2	1	p	13.0	24	13	116	2.5	1.5	1.3	5.2	10.2
	41,596	0	44	1	1		4.0	37	40	0
	46,386	23	42	4	1		6.8	13		117	12	2	1.0	7.1	12.5
a	48,580	5	22	1	1		11.5	25	35	96	1.5	1	1.7	2.7	5.8
	51,313	10	30	3	1		6.5	42		114	3	1.5	1.2	3.0	20.0
	51,689	9	34	4	1		4.0	30	30	98	2.5	1.5	1.3	1.7	12.8
	56,318	37	81	10	3		1.9	10		90	20	2	1.0	4.0	21.3
a	56,611	5	21	1	1	$p \pi$	5.4	25	42	100	1.5	1	1.7	1.2	5.8
	57,384	12	28	3	1		5.3	7		126	5.5	1.5	1.1	3.2	4.2
a	57,424	2	9	1	1		1.5	26	26	99	1	1	3.7	0.14	2.4
	60,186	14	61	5	2		5.5	7	24	80	4.5	2	1.1	3.9	5.0
	60,484	15	54	4	2		2.8	10		90	5	2	1.2	5.1	11.3
	61,331	13	27	4	1		1.1	7		130	6	1.5	1.1	0.73	4.6
a	61,582	2	10	1	1	π	13	16		90	1	1	3.7	1.2	1.5
	61,759	10	35	3	1	p	2.7	7		102	3	1.5	1.2	1.2	3.2
	62,220	22	54	2	1.5		3.7	8		99	9.5	2.5	1.1	3.7	8.0
a	62,419	5	15	1.5	1.5	π	23	45		128	2	1	1.6	6.5	9.5
b	73,834	3	32	1	1		4.1	40		46	1.5	2	1.8	0.90	8.7
	75,535	8	23	2	1	p	5.0	9	47	122	2.5	1	1.3	2.0	3.6
	77,217	14	32	3	1		13.2	18		119	5.5	1.5	1.1	8.6	11.7
	77,242	6	8	10	1.5		2.8	7	149	166	12	1.5	1.1	2.2	5.5
	77,771	18	52	4	1.5		2.8	11		98	7	2	1.1	2.3	9.2
	80,322	26	32	6	1		11.2	22	34	137	20	2	1.0	13.5	26.5
$\pi+\pi$ $m=800$															
	38,385	12	21	1	1.5		14.2	23.5	24	68	1	1	2.6	2.0	3.2
	38,521	14	19	1	1		13	22	13	78	1	1	2.6	1.8	3.1
	40,881	25	45	1	1		4.3	24	35	68	1	1.5	1.4	1.4	7.8
	41,610	20	72	1	4	π	17.6	43	15	46	1	1.5	1.3	7.4	18.1
	43,891	5	6	1	1		12.3	30	39	83	1	1	7.4	0.66	1.4
a	47,698	12	38	1	2	π	2.6	15	34	48	1	1.5	1.8	0.57	3.3
	48,580	5	22	1	1		11.5	25	35	33	1	1.5	2.9	1.4	3.1
	49,310	9	12	1	1	π	3.7	14	13	79	1	1	3.9	0.33	1.2
a	56,611	5	21	1	1	$p \pi$	5.4	25	42	35	1	1.5	3.1	0.61	2.8
a	57,424	2	9	1	1		1.5	26	26	30	1	1	6.3	0.08	1.4
	58,647	10	29	1	1	π	3.5	40		52	1	1.5	2.2	0.61	7.0
a	61,582	2	10	1	1	π	13	16		24	1	1	5.3	0.84	1.0
a	62,419	5	15	1.5	1.5	π	23	45		47	1	1	4.1	1.9	3.8
	72,699	8	18	1	1		10.6	21	29	58	1	1	3.5	1.1	2.2
	73,548	6	12	1	1		8.8	22	33	63	1	1	4.5	0.67	1.7
b	73,834	12	28	1	1	π	9.0	30		58	1	1	2.2	1.5	5.1

^a These observations could be either $p+\pi$ or $\pi+\pi$ decays from the standpoint of ionizations.

^b These observations form a V^0 pair.

tained by setting $\phi^* = \pi/2$, $\gamma\beta = 1$, and choosing for p_2^* the value which it has when $p_1^* = p_2^* = p_\nu^*$. For the masses listed above, that value is 240 electron masses. Such a plot is given in Fig. 4. Note that the conservation requirements impose a cutoff on θ_1 (i.e., on β_1^*) before $dm/dE^*(\theta_1)$ reaches its maximum. Also shown in a similar plot for $p_2^* = 460$ electron masses, the largest value it can take on. It is clear that the most likely values of $\tan\theta_1$ are of the same order of magnitude as its upper limit.

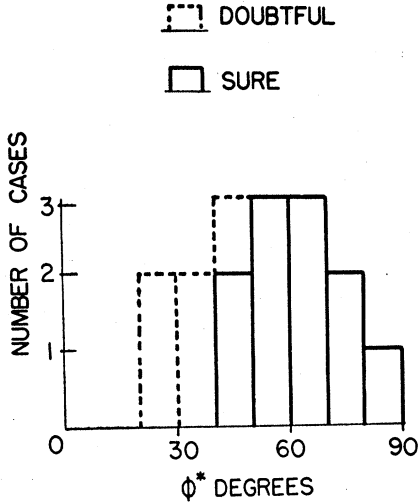
Since that upper limit corresponds to two-particle decay ($p_\nu^* = 0$), the range of most probable values of θ_1 determined by a certain V^0 momentum under the assumption of three-particle decay lies close to the value of θ_1 determined by the same V^0 momentum under two-particle decay. Thus, a given experimental θ_1 distribution gives similar V^0 momentum distributions under both assumptions, and consequently, similar spreads in the angles and ionizations of the decay tracks.

Hence, it would be difficult to use θ_1 measurements to differentiate between the two assumptions.

Another distribution of interest which may be obtained is the distribution in p_ν^* , the momentum of the neutrino in the center-of-mass system. If a three-particle decay process is interpreted as two-particle decay and one attempts to determine the V^0 mass from the experimentally measurable quantities p_1 , p_2 , and θ (the angle between p_1 and p_2), one obtains instead of the true V^0 mass m , a relativistically invariant expression m'^0 :

$$\begin{aligned} m'^2 &= (E_1 + E_2)^2 - (p_1 + p_2)^2 \\ &= (E_1^* + E_2^*)^2 - (p_1^* + p_2^*)^2 \\ &= m^2 - 2m p_\nu^*. \end{aligned}$$

Since actually, if a three-particle decay does exist, with a disintegration energy of order $m/10$ to $m/5$, p_ν^* will be of the order $m/10$ or smaller, and, to a first approxi-


 FIG. 6. Distribution in ϕ^* for $\pi^+\pi^-$ cases.

mation, we will have

$$m' = m(1 - 2p_v^*/m)^{1/2} \cong m - p_v^*.$$

Since histograms of m' (or rather of its equivalent $Q' = m' - m_1 - m_2$) are available, the p_v^* distribution is therefore of some interest. We have

$$\frac{dn}{dE^*} = \frac{2}{\pi \hbar^3} p_1^* p_v^* (E^* - E_1^* - p_v^*) dp_1^* dp_v^* d\Omega''.$$

Thus, p_v^* ranges from 0 to $E^* - E_1^* (= m - E_1^*)$ and maximizes dn/dE^* at $(m - E_1^*)/2$. This is the usual result to be expected in any three-particle decay process involving a neutrino.

Brueckner and Thompson¹² have investigated the distribution in δ , the angle which the V^0 makes with the plane of the proton and meson ($\delta \leq \theta_1$) (an angle which would vanish under the assumption of two-particle decay), and have found a broad maximum at $\delta = 0$. A study of the dependence of dn/dE^* upon the other angles and the momenta has failed so far to reveal any striking characteristics such as might be used to distinguish between two-particle and three-particle decay. In particular, there seems to be no correlation between the directions of the three decay particles in the center-of-mass system if, as indicated by phase space arguments, their momenta tend to be equal in that system. Thus, if one expresses dn/dE^* as a function of θ^* and, say p_2^* , even assuming particle (1) to be very heavy in comparison with particle (2), the distribution in θ^* is not sharp except in the (unlikely) case that p_1^* and p_2^* are much larger than p_v^* ; then, dn/dE^* is maximum at $\theta^* = 180^\circ$. Similar conclusions can be drawn for the other angles.

RESULTS

The data, together with quantities calculated from the data in terms of various decay schemes, are pre-

sented in Table II. We concern ourselves now with the 34 coplanar measurable cases, omitting those where the measurements were uncertain or impossible. In 16 cases the slower particle came off at the smaller angle and therefore, must, have been heavier. Since the particles are not electrons and have a lifetime of order 10^{-8} second or longer (this is deduced from the dimensions of the chamber and the lack of observed decays), the decay particles are either hitherto unknown particles or else must be identified as a proton and a meson (π or μ), respectively. We shall assume a π -meson rather than a μ -meson, because $\pi - \mu$ decays have been observed and π -mesons, as distinguished from μ -mesons, have been identified in a few similar cases elsewhere.^{2,9} We therefore postulate



Observed ionizations in 16 cases then lead to a V_1^0 mass between 2200 and 2400 electron masses. This hypothesis also leads to agreement with observed ionizations in 7 more cases, in all of which both particles travel at minimum ionization. In the remaining 11 cases, however, the hypothesis leads to disagreement with observed ionizations well outside experimental error. All but 2 of those 11 cases involve minimum ionization particles only, and could be accounted for by decay scheme (C) with a V^0 mass of order 2700–2800. The 2 exceptions involve a slower particle (which comes off at the larger angle), and decay scheme (C) cannot explain them at all. We have not attempted to use the ionization estimates in an accurate way. If the observed and calculated ionizations agree to a factor of two, this is considered satisfactory. When an ionization is listed as $1.5 I_{\min}$, it means only that the track looked slightly above minimum, and probably not as much as $3 I_{\min}$, for example.

Following a suggestion due to the Manchester group,² we attempt to explain these 11 cases by postulating a second decay scheme:



A V_2^0 mass of 700 to 900 electron masses can then account for the observed ionizations in all 11 cases, as well as 5 of the 7 minimum ionization cases which could also be accounted for by decay scheme (C). Thus, we have in all 18 cases which can only be explained by scheme (C), 11 cases which can only be explained by scheme (D), and 5 cases which can be explained by either.

We next attempt to determine the V^0 masses more closely. Given any mass value, we can compute a ϕ^* distribution. However, except for 8 cases where one of the decay particles stops in the chamber, we cannot measure masses directly. Other experimental groups,^{2,4,9} working with magnetic fields, have measured them, and we shall begin by using the values which they obtained and by examining the corresponding ϕ^* distribution.

For decay processes (D), the Manchester group²

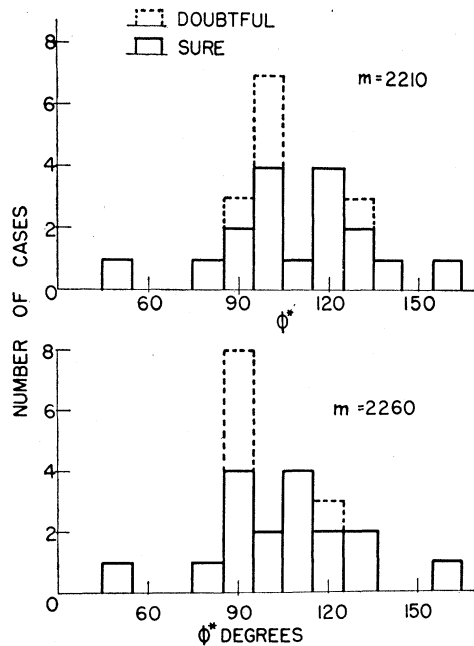


FIG. 7. Distribution in ϕ^* for $p+\pi$ cases.

obtains a V_2^0 mass of 800 electron masses. This value yields the ϕ^* histogram shown in Fig. 6. We have plotted both the 11 cases which can only be explained by decay scheme (D) (solid line) and those 11 plus the 5 which can be explained by either scheme (dotted line). While there are too few observations for the result to be very significant, it can perhaps be concluded that most if not all of the 5 doubtful cases should be accounted for by scheme (C), where, as we shall see, they lead to more probable values of ϕ^* . It should be noted that, since we cannot differentiate between positive and negative decay products, we cannot tell whether ϕ^* is greater or less than 90° . Little more can be said about these data other than that they are compatible with the Manchester assumption. Observed and calculated ionizations, together with the measured angles θ_1 and θ_2 are shown in Table II.

For decay process (C), the Manchester group obtains a V_1^0 mass of 2210 electron masses.² The corresponding ϕ^* histogram is shown in Fig. 7 (dotted line graph includes doubtful cases); and the observed and calculated ionizations are compared in Table II. It is seen that the calculated ionizations are on the whole larger than the observed values (although not outside experimental error; the two worst cases, 46,386 and 62,220, are both "borderline" events so far as accuracy of measurement is concerned) and that an excess of protons seems to be emitted backward in the center-of-mass system of the V_1^0 . Both conditions can be remedied by increasing the V_1^0 mass. Leighton *et al.*⁹ quote two measured mass values for process C, 2170 and 2260. The former leads to somewhat worse disagreement with

our data than does the Manchester figure. The latter improves the situation only slightly (see Fig. 7). Calculations based on a V_1^0 mass of 2350 electron masses have also been carried out for purposes of comparison. This last value is in outright disagreement with the experimental results of all other groups and results are not shown for that reason. A more nearly normal ϕ^* distribution was indeed obtained, however, and the calculated ionizations, although on the light side, agreed with the observed values within the experimental error.

This excess of type (C) decays for which $\phi^* > 90^\circ$ for accepted values of the V_1^0 mass is somewhat puzzling. The cloud chamber tends to select low energy V_1^0 's, since the initial event and the decay must both be contained within a limited volume. However, two independent variables are needed to specify the process in the laboratory system, and we may choose ϕ^* and γm , the V_1^0 energy, to be those two variables. Therefore, for any given V_1^0 energy, the distribution in ϕ^* should still be sinusoidal. It is certainly true that if the V_1^0 is of high energy, and it is required that the proton be above minimum ionization for identification, the distribution will be biased toward events where the proton came out backwards. But, since most of our V_1^0 's are low energy and in addition, the 5 uncertain cases (all of which involve minimum ionization particles only) are included with the 18 "sure" type (C) decays (16 of which involve protons at heavier than minimum ionization), we cannot invoke a bias toward slow protons which would tend to be emitted backwards in the center-of-mass system. Including these 5 cases, we have 17 events with $\phi^* > 90^\circ$ vs 6 events with $\phi^* \leq 90^\circ$ for $m=2210$ and 16 events with $\phi^* > 90^\circ$ vs 7 events with $\phi^* \leq 90^\circ$ for $m=2260$. If anything, adding the 5 uncertain events makes the

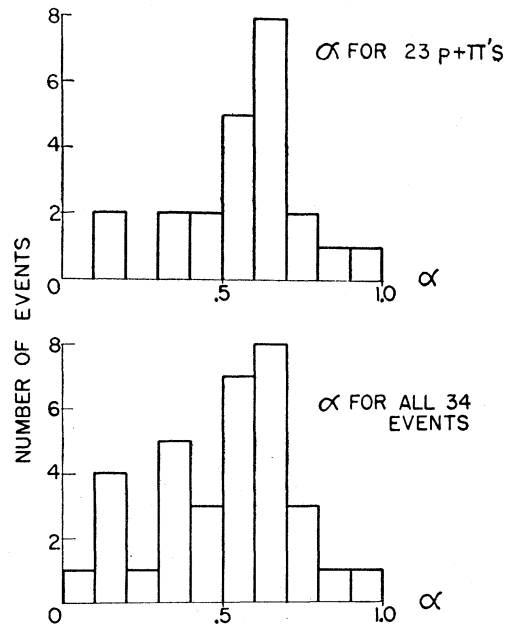


FIG. 8. Distribution in $\alpha = \sin(\theta_2 - \theta_1) / (\sin(\theta_2 + \theta_1))$.

distribution worse (see Fig. 7). Poor statistics or some unknown systematic error in measurement of the angles (e.g., overestimating both θ_1 and θ_2) might explain the asymmetry.

For completeness, we have plotted in Fig. 8 the distribution in α , where²

$$\alpha = \frac{\sin(\theta_2 - \theta_1)}{\sin\theta} = \frac{m_1^2 - m_2^2}{m^2} + \frac{2p^* \cos\phi^*}{\beta_m}$$

Since the average and most probable value of $\cos\phi^*$ is zero, the distribution should center about $(m_1^2 - m_2^2)/m^2$. This is 0.65 for $m = 2260$ and 0.67 for $m = 2210$. Instead, as seen in Fig. 8, the lower values of α predominate and, since θ_1 , θ_2 , and θ are measured quantities, we have thus a fairly direct confirmation of the ϕ^* histograms.

In 8 cases, one or both secondary particles stop within one of the lead plates in the chamber. This allows us to set an upper limit on its momentum, and thereby also on the mass m of the V^0 , by means of transverse momentum considerations and the formulas developed previously. The results are shown in Table III. It is seen that, in 4 of the 8 cases, the maximum V^0 mass is of order 2200 electron masses (only two figures are significant) in agreement with the work of other experimenters referred to above. One of these cases, 56 611, is listed as uncertain on the basis of ionization evidence. However, scattering measurements seem to identify it as a $p + \pi$ decay. Another event, 80,322, is also of some interest, as particle (2), presumably a π -meson traveling at or near minimum ionization, also stops. Its range is no more than 1.4 cm of brass. This would put its momentum at 120 Mev or less, while the transverse momentum balance yields $p_2 = 434$ Mev. Since the particle does not leave the chamber, one is led to the conclusion that some nuclear interaction must have taken place in the brass. This would tend to indicate that particle (2) is indeed a π -meson rather than a μ -meson.

Finally, the momentum distribution for both types of V^0 's have been plotted (Fig. 9). The peak for the V_1^0 with $m = 2210$ comes near $\beta\gamma = 0.6$, and for the V_2^0 , near 2. Since, however, the former is nearly 3 times as heavy as the latter, the actual most likely momenta in

TABLE III. Determination of V^0 mass from range of secondary particle (all cases assumed $p + \pi$).

Observation number	Particle measured	Maximum range cm of Pb	Maximum V^0 mass $\times 10^2 m_e$
46,386	proton	1.5	2.3
51,313	proton	1.5	2.2
56,611	meson ^a	4.0-5.3	2.2
61,331	proton	1.6	2.2
77,217	proton	1.8	2.2
77,242	proton	1.3	2.3
77,771	proton	1.3	2.3
80,322	proton	2.1 ^b	2.5

^a Identified from scattering.

^b Cm of brass.

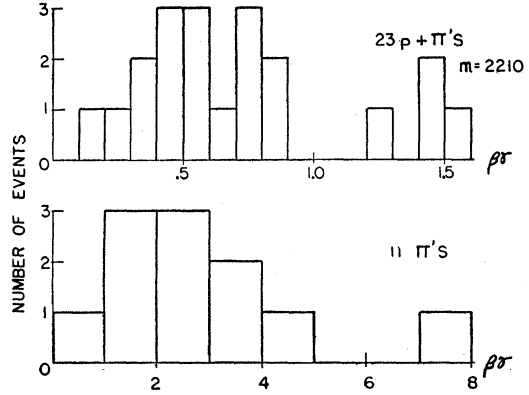


FIG. 9. Distribution in $\beta\gamma$ for all events.

Mev are the same for both particles and of the order 600-800 Mev. The momentum distribution for V_1^0 with $m = 2260$ can be obtained from the plotted distribution for V_1^0 's with $m = 2210$ by multiplying the scale figures by 1.2.

LIFETIMES

The apparatus used required that both the initial event and the decay of the V^0 be contained within the illuminated volume of the cloud chamber before measurements could be carried out. The time of decay in the rest system of the V^0 , t , was given by the measured distance d from initial event to apex of V and by the velocity of the V^0 , which was derived from the angles and depended therefore on the mass and decay scheme assumed: $t = d/\beta\gamma c$, $\gamma = 1/(1 - \beta^2)^{1/2}$. Similarly, the "available decay time" t_a was defined by $t_a = d_a/\beta\gamma c$, where d_a was a distance measured from the initial event along the line of flight of the V^0 to the furthest point where the decay event could have been observed and identified. The i th observation could therefore be characterized by two numbers t_i and t_{ai} , and since necessarily $t_i > t_{ai}$, our selection of data was biased and the mean life, calculated from

$$\bar{t} = \sum_{i=1}^N t_i / N \quad (1)$$

(N = total number of observations), was expected to be smaller than the true value τ .

A first-order correction can be worked out as follows. For every observed decay occurring before t_{ai} , there will be, on the average,

$$\frac{e^{-t_{ai}\tau}}{1 - e^{-t_{ai}\tau}}$$

particles decaying after t_{ai} . These unobserved particles will have a mean decay time $\tau + t_{ai}$, and the sum over t_i 's in Eq. (1) should therefore be replaced by

$$\sum_{i=1}^N \left[t_i + (\tau + t_{ai}) \frac{e^{-t_{ai}\tau}}{1 - e^{-t_{ai}\tau}} \right]$$

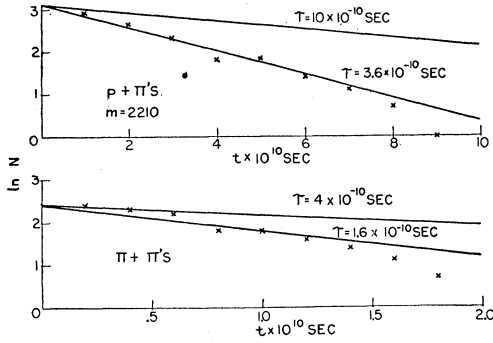


FIG. 10. Plot of measured and corrected lifetimes.

Similarly, the total number of observations is not N , but is

$$N + \sum_{i=1}^N \frac{e^{-t_i/\tau}}{1 - e^{-t_i/\tau}} = \sum_{i=1}^N \frac{1}{1 - e^{-t_i/\tau}}$$

Hence,

$$\begin{aligned} \tau &= \sum_i \left[t_i + (\tau + t_{ai}) \frac{e^{-t_i/\tau}}{1 - e^{-t_i/\tau}} \right] / \sum_i \frac{1}{1 - e^{-t_i/\tau}} \\ &= \frac{1}{N} \sum_i \left[t_i + \frac{t_{ai}}{e^{t_i/\tau} - 1} \right]. \end{aligned} \quad (2)$$

The same formula is obtained¹³ by considering the probability density function for observing N decays occurring at t_i , $i = \dots, N$, observation being conditioned on $t_i \leq t_{ai}$:

$$P(\tau) = \prod_{i=1}^N \frac{e^{-t_i/\tau}}{\tau(1 - e^{-t_i/\tau})},$$

and then making a maximum likelihood estimate of τ , i.e., solving the equation

$$-(\partial/\partial\tau) \ln P(\tau) = 0.$$

By this method, one can also obtain an estimate of the variance

$$\bar{\sigma}^2 = \left\{ \sum_{i=1}^N \left[\frac{1}{\tau^2} - \frac{e^{t_i/\tau}}{\tau^4} \left(\frac{t_{ai}}{e^{t_i/\tau} - 1} \right)^2 \right] \right\}^{-1}. \quad (3)$$

Equation (3) neglects errors in d and in $\beta\gamma c$, the latter being much larger than the former. Taking these errors into account leads of course to a larger variance, as does taking into account the fact that these errors are not the same in all cases. The details have been worked out,¹³ but they are not reported here since it is felt that they cannot have much significance at this time in view of the tentative nature of our conclusions. As seen below, even the minimum statistical variance (3) is sufficiently large so that taking experimental error into account will not make it much larger. Since the plates were only one-half inch thick, we have not corrected

¹³ B. Rankin (private communication).

for particles decaying before they leave the plate in which they were created. We have also neglected the intervening plates since during most of the experiment they were evenly spaced and thus introduce no bias.

For decays of type C, including both sure and uncertain cases, the average decay time in the center-of-mass system, \bar{t} was 3.6×10^{-10} second if $m = 2210$ electron masses, and 3.0×10^{-10} second if $m = 2260$ electron masses. The corresponding corrected mean lifetimes τ , obtained by Eq. (2), were 10×10^{-10} second and 8×10^{-10} second with statistical variance of $\pm 7 \times 10^{-10}$ second and $\pm 6 \times 10^{-10}$ second, respectively. These variances are larger by a factor of three than the statistical error based solely on the limited number of observations, and the large factor is due to the strong bias introduced by the limited size of the cloud chamber. For decays of type D, we include only the 11 sure cases since it was felt that most or all of the 5 uncertain cases were $p + \pi$ decays. The uncorrected average decay time was 1.6×10^{-10} second, and the corrected lifetime was 4×10^{-10} second with a variance of 3×10^{-10} second. A semilogarithmic plot of number of particles not decayed vs time is shown in Fig. 10. The conclusions which can safely be drawn from the data are, therefore, (1) the decays postulated have mean lifetimes of order 10^{-10} to 10^{-9} second; and (2) the lifetime against type C decays may be different from the lifetime against type D decays by a factor which seems to be of order 2, but which may be as large as order 10.

Knowledge of the t_i 's and the t_{ai} 's may also cast some light on the hypothesis of the creation of V^0 's in pairs,¹⁴ which was put forth in an attempt to explain the long V^0 lifetimes by means of universal nuclear coupling constants. If a second V^0 has certainly been created whenever one is observed, the probability for observing the second one is

$$P\left(\frac{T_a}{\tau}\right) = \frac{1}{\tau} \int_0^{T_a} e^{-t/\tau} dt = 1 - e^{-T_a/\tau},$$

where T_a is some average time available for decay in the center-of-mass system. Let us assume that both members of any pair have the same lifetime, the same T_a and are emitted on the average with the same energy. The uncorrected average decay time for either member of the pair is

$$\bar{t} = \int_0^{T_a} t e^{-t/\tau} dt / \int_0^{T_a} e^{-t/\tau} dt,$$

or

$$\bar{t} = \frac{\tau}{1 - e^{-T_a/\tau}} \left[1 - e^{-T_a/\tau} \left(1 + \frac{T_a}{\tau} \right) \right]. \quad (4)$$

We have seen that for either decay scheme

$$\bar{t}/\tau = \frac{1}{2} \quad \text{to} \quad \frac{1}{4}.$$

¹⁴ A. Pais, Phys. Rev. **86**, 663 (1952).

Substituting into (4) and solving for T_a/τ gives 1.25 to 0.55. As would be expected, this is approximately the value obtained for the ratio of the average of the actual t_{ai} 's to τ . Putting it into $P(T_a/\tau)$ gives 0.71 to 0.42, i.e., pairs should be observed in 42 to 71 percent of all cases. Actually 3 pairs were observed in 65 cases. One involved one type C decay and one type D decay. Another involved a type C decay and an unmeasurable event, and the third involved an uncertain case and an unmeasurable event. In at most 10 other pictures, pairs could have occurred and escaped detection, owing to heavy electronic showers, etc. Hence, experimentally, pairs occurred in no more than 20 percent of the cases. This corresponds to $T_a/\tau=0.22$. Since the available decay time is inversely proportional to the $\beta\gamma$ of the V^0 ($t_{ai}=\bar{d}_{ai}/\beta\gamma c$), we can estimate that the more energetic member of the pair must have a $\beta\gamma$ larger than the observed member by a factor ranging from $0.55/0.22=2.5$ to $1.25/0.22=5.7$. If pairs actually are only seen in 10 percent of the pictures, the two values of $\beta\gamma$ differ on the average by a factor ranging from 5.5 to 13. Whether this is a likely or an unlikely situation cannot be said at present.

It has also been proposed¹⁵ that the events which cannot be $p+\pi$ decays should be accounted for by the process

$$V^0 \rightarrow x + \pi, \quad \text{with } m_x = 1000 \text{ electron masses.}$$

The disintegration energy associated with this decay would have to be approximately 175 Mev to agree with observed ionizations. The only known particles with which x might be identified are K or τ -mesons, both of which are thought to have lifetimes of about 10^{-9} second. The question is whether such a short lifetime is compatible with the absence of observed secondary particle decays, at least in the 11 cases which are surely not $p+\pi$ decays. To decide it, we first seek to estimate the time available to particle x for its decay (measured in its own center-of-mass system). This can be done by calculating the average difference between t_{ai} and t_i for the events in question, assuming the above decay scheme, and one obtains about 8×10^{-10} second. Particle x is moving very slowly in the center-of-mass system of the V^0 ($\sim 0.16 c$), and hence this value remains practically unchanged in its own center-of-mass system. If its lifetime is τ_x , the probability of observing 1 decay in 11 events is

$$P = 1 - \exp(-8 \times 10^{-10}/\tau_x) = 1/11;$$

hence, $\tau_x \geq 8 \times 10^{-9}$ second. Hence, the possibility $V^0 \rightarrow K$ (or τ) + π cannot be ruled out as an alternative to decay scheme D. However, it cannot account for all measurable events, for then we would have $P \sim 1/34$ and $\tau_x \geq 2 \times 10^{-8}$ second.

¹⁵ R. B. Leighton, private communication.

C. Analysis of Data Assuming Three-Particle Decay

The identification of some secondary particles as π -mesons makes the process

$$V^0 \rightarrow p + \mu^- + \nu$$

untenable as an explanation of all events. It might still account for some of the events. If there is an elementary fermion with a lifetime 10^{-10} second against decay into a proton and a π -meson, and if there exists a universal four-fermions interaction, it may not be unreasonable to expect $V^0 \rightarrow p + \mu^- + \nu$ decay as a competing process.

One might also advance the single process

$$V^0 \rightarrow p + \pi^- + \nu$$

as a possible explanation for all events. We have seen that five independent variables are needed to specify any such three-particle decay in the laboratory system and, since we only measure two (θ_1 and θ_2), we cannot expect our data to provide any thoroughgoing test of the hypothesis. However, we might expect two quantities, the departure from coplanarity and the spread in V^0 mass values, to behave differently under two- and three-particle decay. So far as the first one is concerned, the angle which the V^0 makes with the $p-\pi$ plane, δ , is less than θ_1 , and therefore less than 20° in nearly all cases. Since, furthermore, its theoretical distribution¹² shows a broad maximum at $\theta=0$ and since our coplanarity measurements are only accurate within 5° , our results (34 coplanar cases vs 7 noncoplanar ones) cannot be used to differentiate between two- and three-particle decay.

CONCLUSIONS

Our conclusions may be summarized as follows:

(1) If the 34 coplanar cases are interpreted as two-particle decays, one particle was heavier than the other in 18 cases, and the measurements on angles, ionizations, and scattering agreed best with the assumption of a $p+\pi$ decay with a disintegration energy of 50-100 Mev. In 11 more cases, angles and ionizations precluded that possibility, but interpretation on the basis of a $\pi+\pi$ decay seemed permissible. Five cases lent themselves to either interpretation from the standpoint of angle-ionization measurements.

(2) The assumption of masses of 2210 and 2260 for the V_1^0 which decays into a proton and a π -meson led to calculated ionizations on the whole too high, but not outside experimental error, and to values of ϕ^* predominantly larger than 90° . Assuming a mass of 800 for the V_2^0 which decays into two π -mesons led to ionizations in agreement with experiment. The ϕ^* distribution was not significant.

(3) A search for experimental bias failed to turn up any decisive reasons for the anomalous ϕ^* distribution. Statistics are poor, however.

(4) The lifetime of the V_1^0 is $(10 \pm 7) \times 10^{-10}$ second and the lifetime of the V_2^0 is $(4 \pm 3) \times 10^{-10}$ second. The errors given are statistical variances, not probable errors, and the calculated values depend quite strongly on the assumed mass of the unstable particle. If the V_2^0 actually decays into a π -meson and a meson of intermediate mass,^{15,16} which would be quite consistent with our data, the lifetime would of course be different.

(5) Three pairs were observed. Only one allowed classification of both its members, one of which turned out to be a V_1^0 and the other a V_2^0 . This frequency of ob-

¹⁶ Report from Copenhagen Conference, June, 1952.

servation contradicts the hypothesis that V^0 's are created only in pairs, unless one V^0 usually has a value of $\beta\gamma$ from 5 to 10 times as large as the other.

(6) The data do not preclude interpretation by means of a three-particle decay scheme, one of which would be a neutrino.

It was not possible to deduce from the angle between the decay plane and the plane of the V^0 and the primary whether or not the V^0 was consistently emitted with a high angular momentum. Nor was it possible to connect the type of V^0 emitted with the type of primary causing the initial event.

Enhancement of the Green Continuum of Hg by a Rare Gas

C. KENTY AND D. A. LARSON*

Lamp Development Laboratory, General Electric Company, Nela Park, Cleveland, Ohio

(Received September 5, 1952)

The green continuum of Hg vapor in a low current, positive column discharge has been found to be greatly enhanced by the presence of a considerable pressure of a rare gas (e.g., 50-mm argon). The effect is most striking for lower Hg pressures (e.g., at 50°C). At 215°C the light efficiency of the continuum reaches 41 lu/w. The continuum extends from 4000 to 6400Å; its maximum occurs at 5130Å at 115° and shifts toward the violet at higher temperatures. Very small amounts of gas impurity, e.g., 40 parts per million of N₂ increase the brightness and also the voltage; larger amounts, e.g., 150 ppm N₂, quench the brightness almost completely.

THE green and ultraviolet continua of Hg as excited in a low current discharge were first studied by Rayleigh.¹ Volkringer² excited the bands with an electrodeless discharge. The requisites for strong continua are a low current (~ 1 ma) and an elevated Hg pressure (e.g., 200°C).

We have found that the addition of a rare gas (e.g., 43-mm argon) brings out the green, so-called 4850, band strongly at as low as 60°C (hot cathode, $\frac{1}{2}$ -ma positive column, $1\frac{1}{2}$ -inch tube). At 100°C the line spectrum is nearly gone (see Fig. 1, curve *A*). Without the argon, curves *B* and *C* show that the continuum is very weak relative to the lines at 100°C and only moderately strong at 180°. 4916 and 5770-90 tend to persist. Curve *D* shows the continuum excited optically.

Approximately true light intensity distributions for two different temperatures are shown by Fig. 2. They agree sufficiently with Volkringer's² distribution, and show the band extending from 4000 to 6400Å, much further than is commonly recognized. At 115° the maximum is at 5130Å and shifts toward the blue at higher temperatures.

The brightness of the continuum increases rapidly with Hg temperature up to $\sim 210^\circ$, where arc con-

striction sets in and the lines appear. Thus with 55-mm argon the brightness of a 0.25-ma discharge increased 250-fold from 75 to 215°. Meanwhile the voltage rose from 115 to 470 (arc length 10 cm). The light efficiency of the discharge at the higher limit was measured as 41 lu/w.

From 10 to 60 mm argon and, e.g., at 160°C, the brightness and voltage increase roughly in proportion to p ; below 10 mm the brightness decreases rapidly.

The other rare gases yielded qualitatively similar results; Xe in particular gave about the same efficiencies as argon.

The brightness is very sensitive to impurities. So far, and unless otherwise stated, all results deal with "spectroscopically pure" argon containing 30-50 parts per million of N₂. Removal of most of this N₂ was found to lower the brightness to less than half and decrease the voltage 25 percent. Maxima in both brightness and voltage occur around 50 ppm N₂; beyond this the brightness drops rapidly to a few percent at 150 ppm N₂. A drop in voltage beyond the maximum may be due to one or more of several causes not discussed here. The initial rise in brightness is closely related to the increase in voltage whatever the impurity (e.g., H₂O, CO₂).³

With a well-developed continuum (100°C), strong

* Now of Research Laboratory, Westinghouse Electric Corporation, Bloomfield, New Jersey.

¹ Lord Rayleigh, Proc. Roy. Soc. (London) **A114**, 620 (1927).

² H. Volkringer, Ann. phys. **10**, 14, 15 (1930).

³ C. Kenty, Phys. Rev. **80**, 95, 96 (1950).